Improved current spreading in 370 nm AlGaN microring light emitting diodes

H. W. Choi[a] and M. D. Dawson
Institute of Photonics, University of Strathclyde, Glasgow G4 0NW, United Kingdom

(Received 6 August 2004; accepted 6 December 2004; published online 28 January 2005)

The electrical and optical characteristics of a 370 nm AlGaN light-emitting diode based on a microring geometry is presented. By structuring the light emission area into an interconnected array of microscale rings, current spreading in the *n*-type cladding layers is improved. A reduction of differential series resistance is observed, and the device saturates at a higher current as the carriers are injected efficiently and uniformly across the junction areas. As a result, optical output power from the microring light-emitting diode is improved compared to a conventional device of broad area geometry. © *2005 American Institute of Physics*. [DOI: 10.1063/1.1861130]

With a wide range of potential applications, the development of ultraviolet (UV) light emitters based on GaN has become a research area of intense interest. Phosphors, excited by a 350 nm nitride light-emitting diode (LED), have been demonstrated as white light sources with high efficiency and accurate color rendering.[1] Devices emitting at a wavelength of 365 nm (i-line) can serve as illumination sources in photolithography systems.[2] At even shorter wavelengths (of down to 280 nm), these light sources can also be used for chemical and biological agent detection/analysis purposes.[3]

In order to achieve emission in the UV region, quantum wells based on AlGaN materials are commonly employed. However, AlGaN based LEDs exhibit inferior emission capabilities compared to their InGaN visible-light emitting counterparts. Large differences in lattice parameter and thermal expansion coefficient between AlGaN (especially at higher Al compositions) and GaN results in materials with poor crystal quality. Unlike InGaN-based visible LEDs, AlGaN-based LEDs are much more sensitive to the dislocation density, suggested to be due to the lack of an exciton-localization effect.[4]

In order to improve crystalline quality in the LED structure, AlGaN/GaN superlattices (SLS) are typically incorporated as cladding layers. SLS are used for enhanced doping activation[5] and reduction of line defect density,[6] at the expense of possible degraded transport properties. This implies that LEDs fabricated using such materials are likely to suffer from serious current crowding effects, and thus nonuniform light emission.

In this letter, we report on the characteristics of an AlGaN based LED adopting the microring mesa geometry, which exhibits improved electrical and optical characteristics. In our previous report, we have shown that it is possible to achieve a twofold increase in optical power output per equivalent emitter area from an InGaN based microring LED emitting at 470 nm light output compared to a broad-area (BA) LED. We attributed the enhanced emission to a combination of improved light extraction (due to greater surface area to volume ratio) and reduced reabsorption in the LED structure. These arguments are still valid for UV devices, except that the microring geometry offers an additional and important benefit over BA devices: improved current spreading.

Our device structure was deposited over 2-in. *c*-plane sapphire substrate by metal organic chemical vapor deposition (MOCVD).[4] The structure consists of a 5 nm undoped GaN buffer over the substrate, followed by 2.3 μm of undoped GaN and 1.4 μm of *n*-doped GaN. On top of the 200 nm 50-period *n*-doped AlGaN/GaN SLS cladding layer, a 7-period multiquantum well (MWQ) active region was grown. The MQW consist of a 2 nm InGaN ($\mathrm{In}\sim 0.05$) well and a 10 nm AlGaN ($\mathrm{Al}\sim 0.2$) barrier. The MQWs are capped with a 100 nm 50-period Mg-doped AlGaN/GaN SLS cladding layer and a 20 nm Mg-doped GaN as a contact layer.

Microring LEDs refer to devices where the mesas are replaced by an interconnected network of microring elements, formed by inductive-coupled plasma (ICP) etching. In this device, the micro-ring network consists of a hexagonal array of 12×19 elements each having an external (internal) diameter of 20 μm (12 μm), corresponding to an effective junction area of $\sim 6.9\times 10^{-2}$ mm^2. Details of the fabrication

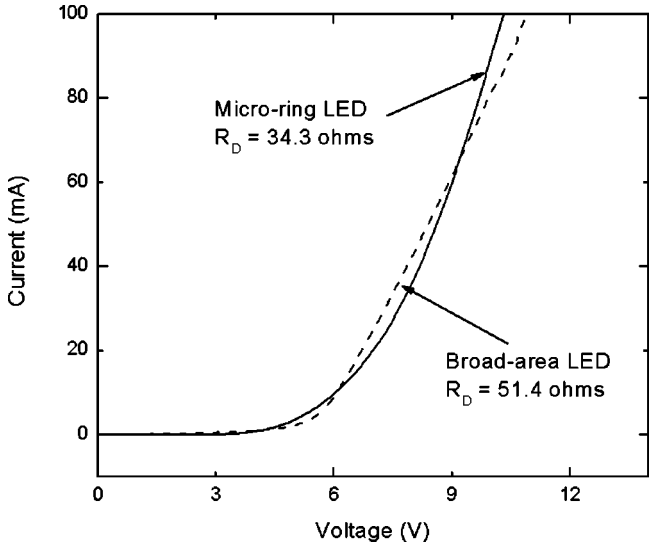

FIG. 1. *I–V* plots for the UV BA and microring LEDs.

[a]Electronic mail: hwchoi@eee.hku.hk; present address: Department of Electrical and Electronic Engineering, University of Hong Kong, Pokfulam Road, Hong Kong.

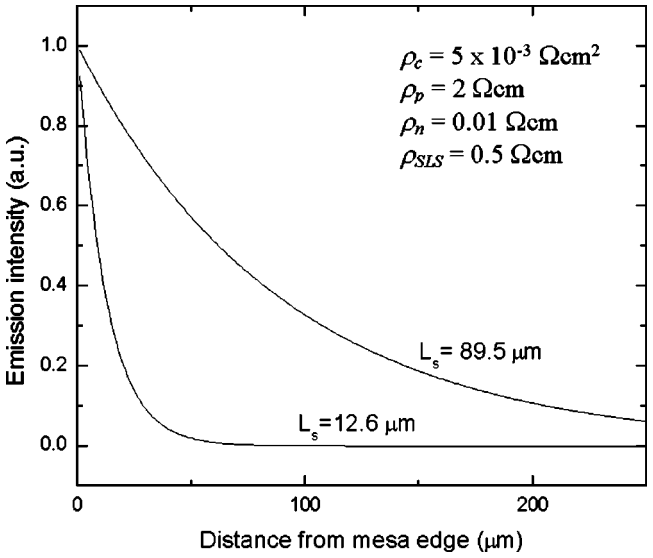

FIG. 2. Theoretical emission intensity vs distance from the edge of the LED.

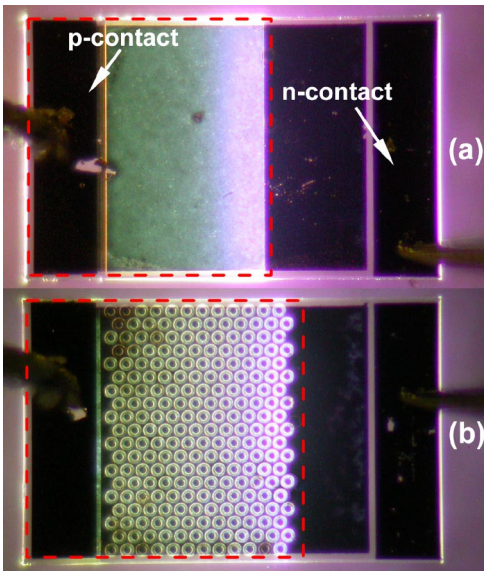

FIG. 3. (Color online) Microphotograph of the (a) BA LED and (b) microring LED operated at 50 mA. The current spreading metal regions are highlighted in dotted lines.

process can be found in Ref. 6. For comparison purposes, a conventional BA LED is fabricated from the same wafer. The $I-V$ characteristics of the devices were measured with an HP4155 parametric analyzer, while the optical power measurements were made on bare chips in a probe-station configuration with a calibrated power meter having a Si detector (detector area of 10 mm diameter) placed 10 mm above the device.

The $I-V$ characteristics of the micro-ring LED and the BA LED are shown in Fig. 1: at lower injection currents (of <40 mA), the microring LED has inferior electrical characteristics. It turns on at 6.94 V (compared to 5.83 V for the BA LED), and has a leakage current (at $V=-3$ V) of 70.48 μA (compared to 0.75 μA for the BA LED). Note that due to the smaller junction area of the microring LED, it is also operating at a higher current density, which accounts partially for the higher leakage current. Nevertheless, in the high-injection current regime, the microring LED has a lower differential series resistance of 34.3 Ω (compared to 51.4 Ω for the BA LED). Such differences can be attributed to the distinctive geometry of the microrings. The higher turn-on voltage is a result of current injection through the micron-scale contact, where contact resistance is higher.[7] The reduced differential series resistance can be attributed to improved current spreading.

In our UV device structure, the n-type SLS cladding layer gives rise to a high lateral resistance and thus current crowding occurs at the mesa edges. The current density as a function of the distance from the n-contact is given by[8]

$$J(x) = J(0)\exp\left(-\frac{x}{L_s}\right), \tag{1}$$

where $J(0)$ is the current density at the p-type mesa edge and L_s is denoted as the current spreading length, which is given by

$$L_s = \sqrt{(\rho_c + \rho_p t_p)t_n/\rho_n}, \tag{2}$$

where ρ_c is the specific contact resistance of the p-contact, ρ_p, ρ_n, t_p, and t_n are the resistivities and thicknesses of the p and n-type cladding layers, respectively. In the device structure, the n-type cladding layer consists of a 50-period AlGaN/GaN SLS on top of a 1.4 μm n-type GaN layer ($n \sim 3\times10^{18}$ cm^{-3}). Due to parallel conduction, current flow cannot be determined by the n-GaN layer alone. To further complicate matters, the mechanisms for lateral and perpendicular transport in the SLS layer are different, giving rise to different lateral and perpendicular resistivities. Recently, Waldron *et al.* reported on the characterization of a 30-period AlGaN/GaN SLS which has a resistivity 6.6 times higher than bulk material.[9] Considering all these factors, we have estimated L_s to be $\sim$12.6 μm, using parameters listed in Fig. 2, which also shows the plot of relative emission intensity versus distance in a BA LED. The microphotograph in Fig. 3(a), showing the operation of a UV BA LED illustrates this phenomenon, where light emission is observed to be confined to one edge of the 250 μm$\times$400 μm mesa LED.

By separating the light emission region into multiple microring elements, the SLS cladding layers in each microring are no longer interconnected, and thus do not play a role in

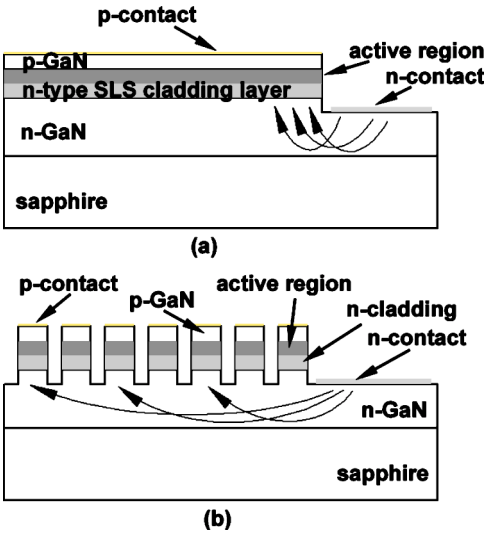

FIG. 4. Schematic diagram illustrating current flow (and current crowding effects) in (a) BA LED and (b) microring LED.

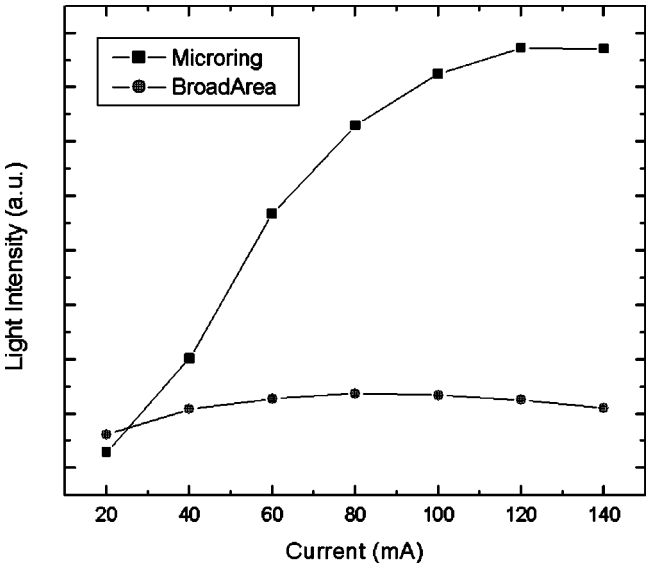

FIG. 5. Plot of light output power as a function of current for the BA and microring LEDs.

current spreading. Schematic diagrams illustrating the difference in current conduction in the BA and microring LEDs are shown in Figs. 4(a) and 4(b). In the microring LED, *p*-type GaN and SLS cladding materials is partially removed (between the microrings), forcing the current to flow along the *n*-type GaN layer which offers better current spreading due to a lower resistivity compared to parallel conduction along the *n*-GaN and SLS layers. Current spreading length in the *n*-GaN layer is calculated to be $\sim 90\ \mu$m, 8 times higher than in the BA LED. This value is still relatively low compared to an InGaN based longer-wavelength LEDs. The operation of a microring LED is shown in Fig. 3(b). Although light emission is still stronger near the edge area, it is much more uniform compared to a BA LED.

With uniform light emission across the device, higher optical outputs can be expected. As seen from the plot in Fig. 5(a), the output power saturates at 80 mA for the BA LED. However, in the equal active area microring LED, the power saturates at a much higher current of 120 mA, and emits 3 times more optical power at this current compared to the BA LED, despite being 30% smaller in junction (light emission) area. This trend is similar to that of the multifinger-design proposed by Chitnis *et al.*,[10] where the increase in saturation current was explained in terms of improved differential series resistance (thus reduced current crowding) and a heat-sinking effect.

In summary, a 370 nm LED based on a microring geometry has been demonstrated. Compared to an equal active area reference broad area LED, the microring device exhibits lower differential series resistance, higher emission uniformity due to improved current spreading, and the optical power saturates at a higher current of 120 mA compared to 80 mA in the BA LED. Coupled with increased extraction efficiency and reduced absorption, the micro-ring LEDs offer a means of improving optical output characteristics.

The authors would like to thank Dr. A. C. Bryce for support on metal deposition in this work.

[1]T. Mukai, M. Yamada, and S. Nakamura, Jpn. J. Appl. Phys., Part 1 **38**, 3976 (1999).
[2]D. Morita, M. Sano, M. Yamamoto, T. Murayama, S. Nagahama, and T. Mukai, Jpn. J. Appl. Phys., Part 1 **41**, 1434 (2002).
[3]Y.-L. Pan, V. Boutou, R. K. Chang, I. Ozden, K. Davitt, and A. V. Nurmikko, Opt. Lett. **28**, 1707 (2003).
[4]T. Wang, Y. H. Liu, Y. B. Lee, Y. Izumi, J. P. Ao, J. Bai, H. D. Li, and S. Sakai, J. Cryst. Growth **235**, 177 (2002).
[5]E. L. Waldron, J. W. Graff, and E. F. Schubert, Appl. Phys. Lett. **79**, 2737 (2001).
[6]H. W. Choi, M. D. Dawson, P. R. Edwards, and R. W. Martin, Appl. Phys. Lett. **83**, 4483 (2003).
[7]H. W. Choi, C. W. Jeon, M. D. Dawson, P. R. Edwards, R. W. Martin, and S. Tripathy, J. Appl. Phys. **93**, 5978 (2003).
[8]X. Guo and E. F. Schubert, Appl. Phys. Lett. **78**, 3337 (2001).
[9]E. L. Waldron, Y.-L. Li, E. F. Schubert, J. W. Graff, and J. K. Sheu, Appl. Phys. Lett. **83**, 4975 (2003).
[10]A. Chitnis, V. Adivarahan, M. Shatalov, J. Zhang, M. Gaevski, W. Shuai, R. Pachipulusu, J. Sun, K. Simin, G. Simin, J. W. Yang, and M. A. Khan, Jpn. J. Appl. Phys., Part 1 **41**, L320 (2002).